Human-Robot Cooperative Manipulation Using a Virtual Nonholonomic Constraint

Tomohito Takubo[1], Hirohiko Arai[2], Yasuo Hayashibara[3] and Kazuo Tanie[12]

[1] University of Tsukuba, 1-1 Tennodai, Tsukuba, Japan

[2] The National Institute of Advanced Industrial Science and Technology, AIST Tsukuba East, 1-2-1 Namiki, Tsukuba, Japan

[3] Toin University of Yokohama, 1614 Kurogane-cho, Midori-ku, Yokohama, Japan

Email: t-takubo@aist.go.jp

Abstract

A robotic assistance system is presented which enables a human to handle unwieldy long objects by providing only one point of support. The robot grasps one end of the object and helps the human operator carry it at the other end. The proposed control method uses a virtual nonholonomic constraint. The movement of the object is constrained as if it were being carried on a wheel attached to the object. This method prevents the object from slipping sideways and simplifies the carrying operation. In spite of the constraint, the object can reach any position and orientation due to the nonholonomy. Cooperative manipulation in a horizontal plane is considered first, and then it is extended to 6-dof manipulation in 3-D space. Experimental results show that an operator can easily handle a long object when aided by the robot.

Keywords: Human-robot cooperation, Cooperative manipulation, Virtual nonholonomic constraint, Impedance control

1 Introduction

Most robots are typically used for simple, repetitive tasks in environments isolated from humans. There is increasing demand for human-friendly robot technologies with which robots could collaborate with humans sharing the same workspace. This would expand robot applications from factory automation to such areas as construction work, shipping services, home and office tasks. We will deal here with human-robot coordinated manipulation since object handling is still a typical robot task. The objective of our research is illustrated in **Fig. 1**. The human operator and the robot together hold a long object, and the robot helps the operator carry the object by sharing the operator's load.

Large or long objects are usually difficult to support by grasping only a single point. Such objects are easier to handle when two persons each hold an end and share the load, rather than when one person alone tries to grasp near the object's center of mass. It would be useful if the second human could be replaced by a robot, and the operator and robot could support separate points to manipulate the object.

To simplify our system, we have constructed a controller that uses only the signals from a wrist force sensor and the joint angle sensors of the robot arm. Visual and auditory information, which would require complicated systems for image processing and voice recognition, have not been utilized. We have also excluded intelligent processing for understanding human intention and task planning. We aimed to build a robot system that would be a simple tool that the operator could manage easily, rather than create an autonomous agent comparable to a human assistant.

Previous studies on assisting human force using a robot have investigated an "Extender" or "Power assist" [1, 2, 3]. The robot arm has two force sensors

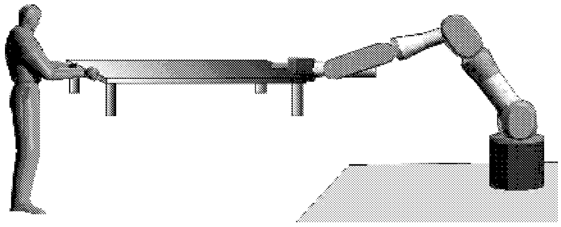

Fig. 1: Human-robot cooperative manipulation

at the wrist that measure the forces exerted by the human operator and the load. The operator's force is amplified by the joint actuators. This method is useful when the load can be grasped at a single point.

On the other hand, in the cooperative task shown in **Fig. 1**, the operator directly contacts the object and the force on the object by the operator cannot be measured independently. Although the operator's force can be estimated if the inertial parameters of the object are known accurately, this is impractical in real-world applications. Moreover, since the force sensor cannot distinguish between external disturbances and the operator's force, it might be dangerous to amplify the estimated force. Therefore, it is difficult to simply extend such a method to the cooperative manipulation described in this paper.

Different approaches for human-robot collaboration have also been proposed in which the robot is used for guiding the object's movement on a pre-planned path. In Refs. [4, 5], nonholonomic mechanisms have been utilized for such a passive motion guide. In these approaches, the human operator pushes or pulls the object along the prescribed path. The object is allowed to move in one degree of freedom, and the path is assumed to be unchanged during the task.

There have also been several research studies on human-robot cooperative manipulation based on impedance control [6, 7, 8] in which the robot is given a virtual impedance and the object follows the force of the human operator. However, it is difficult to apply large torque at the end of a long object and the force the operator exerts is mainly translational. Though axial translation is easy, the rotation and normal translation causes *sideslip* of the object and complicates the manipulation (**Fig. 2 (a)**).

We propose a method that solves this problem by assigning a virtual nonholonomic constraint at the robot hand, which is equivalent to a wheel being attached to the object in the axial direction (**Fig. 2 (b)**). This constraint suppresses the sideslip of the object. By restricting the robot's movement, we have simplified the object's behavior and made it easy for the operator to steer. Nevertheless, the object can reach an arbitrary position and orientation without additional procedures such as changing the constraint conditions.

The rest of this paper is organized as follows. In Section 2, cooperative manipulation in a horizontal plane is considered. Also, the concept of the virtual nonholonomic constraint is proposed, and the control law to realize the constraint is presented. In Section 3, the proposed method is extended to manipulation in 3-D space. The control law for the cooperative manipulation is implemented to a real robot and experimentally verified.

2 Cooperative Manipulation in Horizontal Plane

First of all, we will present a method for manipulating the object in a horizontal plane. We then propose the virtual nonholonomic constraint equivalent to a wheel at the robot hand and also show that the object can reach any position and orientation. Then the control law for the virtual constraint of the robot arm is designed. We implement the control law in a real robot and demonstrate that a human and the robot can cooperatively carry a long object in the horizontal plane.

In our previous study [9], we proposed a control method for the cooperative manipulation of a long object in a vertical plane which was inspired by human cooperative behavior. The basic control scheme consisted of impedance control in the horizontal movement, free rotation at the robot wrist, and keeping the object horizontal during vertical movement. The operator and robot equally shared the gravitational load irrespective of the mass and length of the object. By combining that method with the one proposed here, cooperative manipulation in a 3-D space can be achieved.

2.1 Virtual nonholonomic constraint

2.1.1 Constraint equivalent to virtual wheel

The sideslip in **Fig. 2 (a)** occurs because the impedance parameters are uniform and the object can

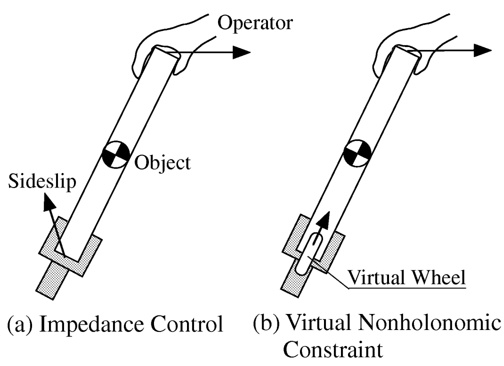

Fig. 2: Cooperative manipulation of long object

move in any direction. It is preferable to limit the direction in which the object can move so that the operator's force and the object's movement have a simple relation. Then the operator can intuitively understand the object's behavior.

Humans often carry a load on a cart with fixed passive wheels such as a wheelbarrow, pushcart or baby carriage. The movement of these carts involves a nonholonomic constraint, i.e., the direction of mobility is restricted by the wheels. The cart can move in a direction tangential to the wheel but cannot move in the normal direction unless the wheels slip sideways against the friction of the floor. Regardless of such a constraint, the cart can in fact finally reach any desired position along an appropriate path. In spite of the difficulty of control in nonholonomic systems, humans generally have the skills to steer these types of carts from their daily experience.

If the object of the human-robot cooperative manipulation were to have the same behavior as the cart, the operator could intuitively understand the response of the object and carry it easily to a desired position. For this purpose, we propose a virtual nonholonomic constraint equivalent to a wheel at the robot hand in the axial direction (**Fig. 3**). In other words, the translational velocity at the robot hand is restricted only in the axial direction. This method provides the following merits.

- The operator can manipulate the object as easily as a fixed wheel cart since the object will not slip sideways in the normal direction.
- The operator only needs to apply translational force to the object for positioning. The bending stress of the object is reduced as it is not necessary to apply torque.
- The controllability of the system is guaranteed due to the nonholonomic constraint, and the object can reach any position and orientation.

2.1.2 Controllability

Figure 3 shows the model of the object under the virtual nonholonomic constraint. The operator holds the object at H: (x_h, y_h) and the robot grasps it at R: (x_r, y_r). The length of the object is L and its orientation is θ. The nonholonomic constraint condition with which the virtual wheel will not slip sideways is represented as

$$\dot{x}_r \sin\theta - \dot{y}_r \cos\theta = 0. \qquad (1)$$

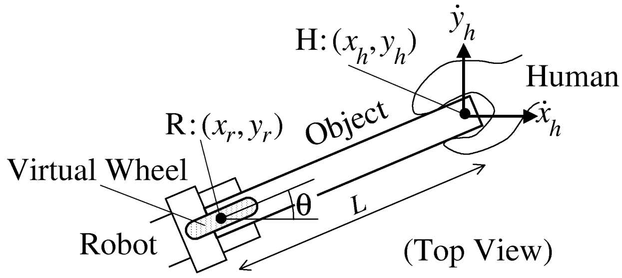

Fig. 3: Virtual nonholonomic constraint

The object can translate only in the axial direction, and can rotate around R. It can also move along a smooth curve continuously changing its direction tangential to the curve at R. The object has the same behavior as though it were being supported by a virtual wheel at R. The operator can manipulate it to a desired position and orientation using the same skills as when steering a cart.

Both ends of the object are kinematically related as

$$\begin{cases} \dot{x}_h &= \dot{x}_r - L\dot{\theta}\sin\theta \\ \dot{y}_h &= \dot{y}_r + L\dot{\theta}\cos\theta. \end{cases} \qquad (2)$$

The state equation of the system is formulated from Eqs. (1) and (2) as follows.

$$\begin{aligned} \begin{pmatrix} \dot{x}_r \\ \dot{y}_r \\ \dot{\theta} \end{pmatrix} &= \begin{pmatrix} \cos^2\theta & \sin\theta\cos\theta \\ \sin\theta\cos\theta & \sin^2\theta \\ -\frac{\sin\theta}{L} & \frac{\cos\theta}{L} \end{pmatrix} \begin{pmatrix} \dot{x}_h \\ \dot{y}_h \end{pmatrix} \\ &= \boldsymbol{g}_1\dot{x}_h + \boldsymbol{g}_2\dot{y}_h. \end{aligned} \qquad (3)$$

This is a drift-free affine system with the configuration of the object as the state variables and the translational velocities of the operator's hand as the inputs.

Now we prove that this system is controllable and can reach any arbitrary state [10]. Lie bracket of the vector fields $\boldsymbol{g}_1$and $\boldsymbol{g}_2$ is calculated as

$$[\boldsymbol{g}_1, \boldsymbol{g}_2] = \frac{\partial \boldsymbol{g}_2}{\partial \boldsymbol{q}}\boldsymbol{g}_1 - \frac{\partial \boldsymbol{g}_1}{\partial \boldsymbol{q}}\boldsymbol{g}_2 = \begin{pmatrix} \frac{\sin\theta}{L} \\ -\frac{\cos\theta}{L} \\ \frac{1}{L^2} \end{pmatrix}. \qquad (4)$$

Then,

$$\det(\boldsymbol{g}_1, \boldsymbol{g}_2, [\boldsymbol{g}_1, \boldsymbol{g}_2]) = \frac{1}{L^2}. \qquad (5)$$

The rank of the distribution composed of $\boldsymbol{g}_1$, $\boldsymbol{g}_2$ and $[\boldsymbol{g}_1, \boldsymbol{g}_2]$ is three, and equals the dimensions of the state space. Hence, the system of Eq. (3) satisfies the Lie algebra rank condition, and is controllable. The object can thus reach any position and orientation.

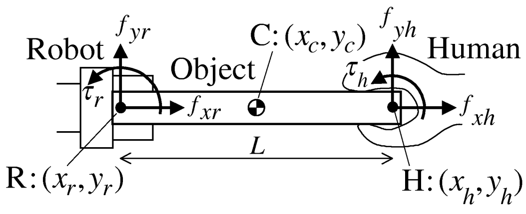

Fig. 4: Impedance control of long object

2.2 Virtual constraint by impedance control

Here we construct the robot control law for virtual nonholonomic constraint based upon impedance control. We assume the robot has a wrist force/torque sensor. First we consider the object behavior for the case in which impedance control is applied at the robot hand. Then we introduce an anisotropic impedance in the hand frame to achieve the virtual nonholonomic constraint.

2.2.1 Object behavior with impedance control

References [6, 7, 8] employ impedance control for human-robot cooperative manipulation. This method assigns virtual impedance parameters, i.e., inertia, damping and stiffness, to the robot and object. The robot follows the human's movement and passively coordinates its force on the object as a load against the operator's force. Here we suppose that this method is being applied to the cooperative manipulation of a long object and that the robot hand is given a virtual impedance.

We will consider a rigid stick on a horizontal plane as the object (**Fig. 4**). M, I and L are the mass, moment of inertia and length of the object, respectively. The center of mass C: (x_c, y_c) is at the middle of the object's length. The robot grasps one end of the object, R: (x_r, y_r), and the human operator grasps the other end, H: (x_h, y_h). The orientation of the object is θ, and the state when θ is zero is considered. The force/torque applied to the object by the operator and by the robot are (f_{xh}, f_{yh}, τ_h) and (f_{xr}, f_{yr}, τ_r), respectively. As the object moves in a horizontal plane, gravity has no influence on the object's movement. Then,

$$\begin{cases} M\ddot{x}_c &= f_{xh} + f_{xr} \\ M\ddot{y}_c &= f_{yh} + f_{yr} \\ I\ddot{\theta} &= \frac{f_{yh}L}{2} - \frac{f_{yr}L}{2} + \tau_h + \tau_r. \end{cases} \tag{6}$$

The robot is given the following impedance comprising mass and viscous friction.

$$\begin{cases} -f_{xr} &= m\ddot{x}_r + b\dot{x}_r \\ -f_{yr} &= m\ddot{y}_r + b\dot{y}_r \\ -\tau_r &= i\ddot{\theta} + c\dot{\theta}. \end{cases} \tag{7}$$

From the kinematic relationship between the center of mass, C, and the robot hand, R,

$$\begin{cases} \ddot{x}_c &= \ddot{x}_r - \frac{L}{2}\dot{\theta}^2 \\ \ddot{y}_c &= \ddot{y}_r + \frac{L}{2}\ddot{\theta}. \end{cases} \tag{8}$$

From Eqs.(6), (7) and (8), the equation of motion of the object can be written as

$$\begin{cases} f_{xh} = (M+m)\ddot{x}_r + b\dot{x}_r - \frac{ML\dot{\theta}^2}{2} \\ f_{yh} = (M+m)\ddot{y}_r + b\dot{y}_r + \frac{ML\ddot{\theta}}{2} \\ \tau_h = (I + i - \frac{ML^2}{4})\ddot{\theta} - (\frac{M}{2} + m)L\ddot{y}_r + c\dot{\theta} - bL\dot{y}_r. \end{cases} \tag{9}$$

The target task for the operator is to manipulate the position of the robot hand and the orientation of the object to a desired configuration. Acceleration in the axial direction, $\ddot{x}_r$, corresponds directly to the operator's force, f_{xh}, and the axial translation is easy. On the other hand, the normal acceleration $\ddot{y}_r$ and the angular acceleration $\ddot{\theta}$ are coupled. Even when the object is translated in the normal direction, the operator must apply a large torque proportional to the length of the object. Similarly, a large torque is required for the operator to compensate for an external force at the robot hand in the normal direction.

However, the operator can mainly exert translational force as it is hard to apply a large torque at the end of the object. In addition, bending stress, caused by the operator's torque, might deform or damage the object if it is fragile. We thus consider a case in which the operator applies no torque to the object and manipulates it only translational forces. When the operator's force τ_h is zero in Eq.(9), the normal acceleration $\ddot{y}_r$ and the angular acceleration of the object $\ddot{\theta}$ are related as

$$(I + i - \frac{ML^2}{4})\ddot{\theta} - (\frac{M}{2} + m)L\ddot{y}_r + c\dot{\theta} - bL\dot{y}_r = 0. \tag{10}$$

Substituting Eq.(10) in Eq.(9),

$$\begin{cases} \ddot{y}_r &= \frac{(I+i-\frac{ML^2}{4})f_{yh} - (I+i+\frac{ML^2}{4})b\dot{y}_r + \frac{MLc\dot{\theta}}{2}}{(M+m)(I+i) + \frac{MmL^2}{4}} \\ \ddot{\theta} &= \frac{(\frac{M}{2}+m)Lf_{yh} + \frac{MLb\dot{y}_r}{2} - (M+m)c\dot{\theta}}{(M+m)(I+i) + \frac{MmL^2}{4}}. \end{cases} \tag{11}$$

The normal force f_{yh} simultaneously generates the acceleration of sideslip, $\ddot{y}_r$, and the angular acceleration,

$\ddot{\theta}$. The rotation and normal translation of the object should be controlled using only one input, f_{yh}, to carry the object to a desired position and orientation.

Small inertia and damping factors should be chosen so that the operator can move the object with minimum force. The object would behave as if it were floating in a gravity-free state. However, the operator does not experience such movement in real life and cannot intuitively anticipate the response of the object. In particular, stopping the object at a desired position and orientation would be a difficult task for the operator. Though larger friction can reduce such behavior, the friction would oppose the operator's force and the load for the human would increase.

2.2.2 Anisotropic impedance in hand frame

The problems in Section **2.2.1** arise because the impedance parameters are uniform and movement in any direction is allowed. We hence simplify the relationship between the operator's force and the object's movement by limiting the direction in which the object can move. The operator can then naturally understand the object's behavior.

Limiting the movement must not degrade the essential goal of the task, i.e., to manipulate the object to a desired position and orientation. For example, an anisotropic impedance in an absolute frame can achieve a virtual constraint and restrict the movement in fixed directions. However, such a constraint is holonomic and the constrained component of the coordinate frame cannot change. Extra procedures for switching the constraint conditions would be necessary to enable the object to reach an arbitrary desired configuration.

Here we consider how to control the robot arm to achieve the virtual nonholonomic constraint described in Section **2.1**. The robot arm is assumed to have a force/torque sensor at the wrist. The X-axis of the end-effector coordinate frame (X, Y) is parallel to the object (**Fig. 5**). (f_{Xr}, f_{Yr}, τ_r) is the force/torque applied from the object to the robot. When the robot does not move in the Y-direction against the force f_{Yr}, the object has apparently the equivalent constraint of a wheel at R in the axial direction. The virtual wheel is passive and frictionless if the robot moves freely following f_{Xr} and τ_r in each direction.

Anisotropic impedance control, in which the impedance parameters depend on the object's orientation, is applied to obtain the constraint. The impedance is assigned in the end-effector frame, not in the fixed absolute frame. Thus the direction of the constraint changes according to the object's orientation as in Eq.(1).

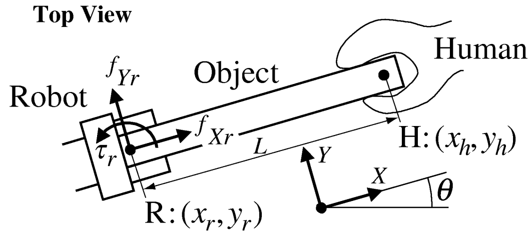

Fig. 5: Impedance control for virtual constraint

The impedance control law, which relates the movement of the robot hand to the force/torque from the object to the robot, is formulated as follows,

$$\begin{cases} f_{Xr} &= m_X \dot{v}_{Xr} + b_X v_{Xr} \\ f_{Yr} &= m_Y \dot{v}_{Yr} + b_Y v_{Yr} \\ \tau_r &= i\ddot{\theta} + c\dot{\theta}. \end{cases} \quad (12)$$

where m_X and b_X are the mass and friction coefficients in the X direction, and m_Y and b_Y are those in the Y direction, respectively. i and c are the moment of inertia and friction coefficient around R. $(v_{Xr}, v_{Yr}, \dot{\theta})$ and $(\dot{v}_{Xr}, \dot{v}_{Yr}, \ddot{\theta})$ are the velocity and acceleration of the robot hand.

(v_{Xr}, v_{Yr}) and $(\dot{x}_r, \dot{y}_r)$ are related as

$$\begin{cases} v_{Xr} &= \dot{x}_r \cos\theta + \dot{y}_r \sin\theta \\ v_{Yr} &= -\dot{x}_r \sin\theta + \dot{y}_r \cos\theta. \end{cases} \quad (13)$$

The constraint in Eq. (1) is realized when $v_{Yr} \approx 0$. Therefore, m_Y and b_Y are given large values to suppress the velocity and acceleration in the normal direction, while the m_X, b_X, i and c values are set as small as possible so that the robot can move almost freely with regard to the axial translation and rotation. Then the virtual nonholonomic constraint equivalent to a wheel attached to the object is achieved.

From Eq. (12), the acceleration of the robot hand is obtained as

$$\begin{cases} \dot{v}_{Xr} &= (f_{Xr} - b_X v_{Xr})/m_X \\ \dot{v}_{Yr} &= (f_{Yr} - b_Y v_{Yr})/m_Y \\ \ddot{\theta} &= (\tau_r - c\dot{\theta})/i. \end{cases} \quad (14)$$

The reference velocity $(v_{XrREF}, v_{YrREF}, \dot{\theta}_{REF})$ of the robot hand can be obtained by integrating Eq. (14). It is transformed to the joint velocity command and sent to the servo controller for each joint. This control law does not include any object parameters, and it is relevant even when the mass and length of the object are unknown.

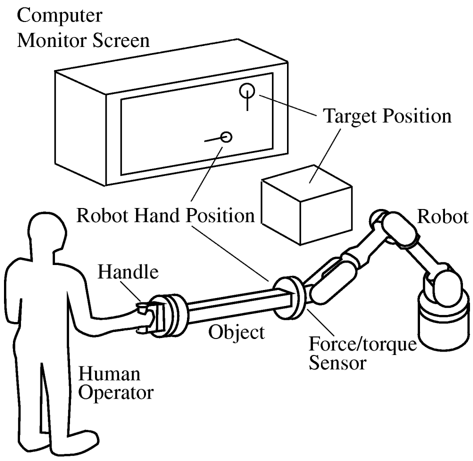

Fig. 6: Experimental setup

Table 1: **Impedance parameters for horizontal plane**

		conventional impedance control	virtual nonholonomic constraint
m_X	[kg]	5.5	5.5
b_X	[kg/s]	20	20
m_Y	[kg]	5.5	100
b_Y	[kg/s]	20	5000
i	[kg m^2]	5.5	5.5
c	[kg m^2/s]	20	20

2.3 Experiments in horizontal plane

We now demonstrate that a human and robot can manipulate a long object cooperatively by implementing the control law discussed in the previous section. **Figure 6** shows our experimental setup. We used a 7-axis industrial robot arm (PA-10, MHI) with a 6-axis force/torque sensor at the wrist, and an electric gripper to grasp the object. A personal computer (CPU: AMD-K5, 166MHz) was used for the controller. The sampling period was 5 msec. The object was an aluminum pipe.

We compared the behaviors of the object using the virtual nonholonomic constraint with conventional impedance control. The impedance parameters we employed in the experiments are listed in **Table 1.** When using the nonholonomic constraint, the mass and friction coefficients in the normal direction are much larger than those in the axial direction.

The operator moves the object from the initial configuration to a desired configuration while watching the marker displayed on a monitor screen. The positioning is complete when the object remains within the target area for 3 seconds. After the operator practices the movement several times for both control methods, the trajectories of the manipulation are recorded.

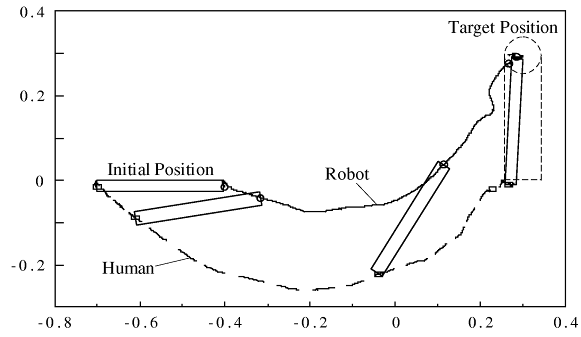

Fig. 7: Trajectory of object (impedance control)

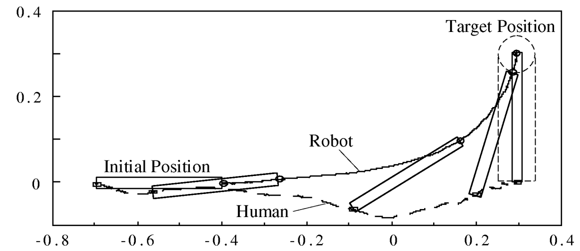

Fig. 8: Trajectory of object (virtual nonholonomic constraint)

Figure 7 and **Fig. 8** show the movement of the object with impedance control and with the virtual nonholonomic constraint, respectively. The trajectory of the robot hand sways due to sideslip when using impedance control, and it is difficult to carry the object to the target position accurately. In contrast, the trajectory with the nonholonomic constraint is smooth and the object can be stably maintained at the desired configuration after positioning.

We then verified that our proposed method enabled the operator to manipulate the object by applying only translational forces. A free-rotating handle was attached to the object to prevent the operator's torque. After the operator pulled the object in the axial direction waving in the normal direction, the velocities at both ends in the normal direction were measured (**Fig. 9**, **Fig. 10**). While the normal velocity of sideslip occurs at the robot hand when using impedance control (**Fig. 9 (b)**), the sideslip is suppressed by the nonholonomic constraint (**Fig. 10 (b)**).

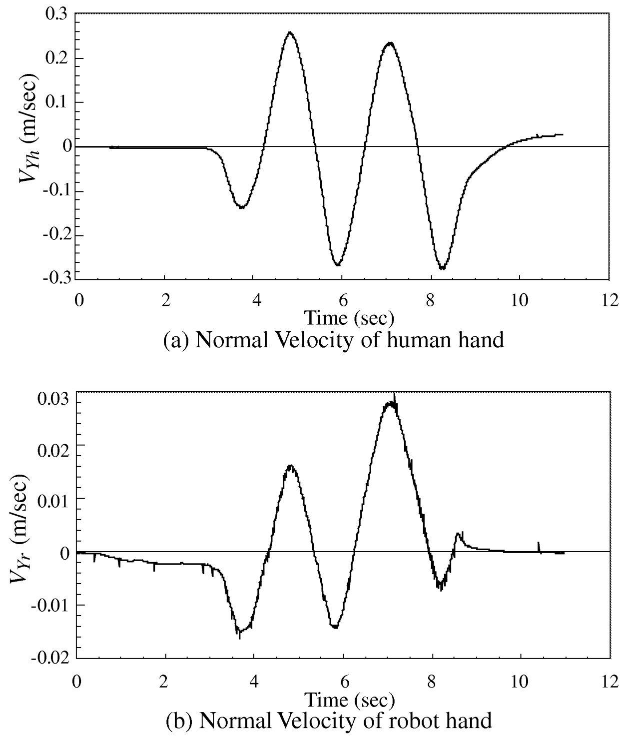

(a) Normal Velocity of human hand

(b) Normal Velocity of robot hand

Fig. 9: Sideslip with impedance control

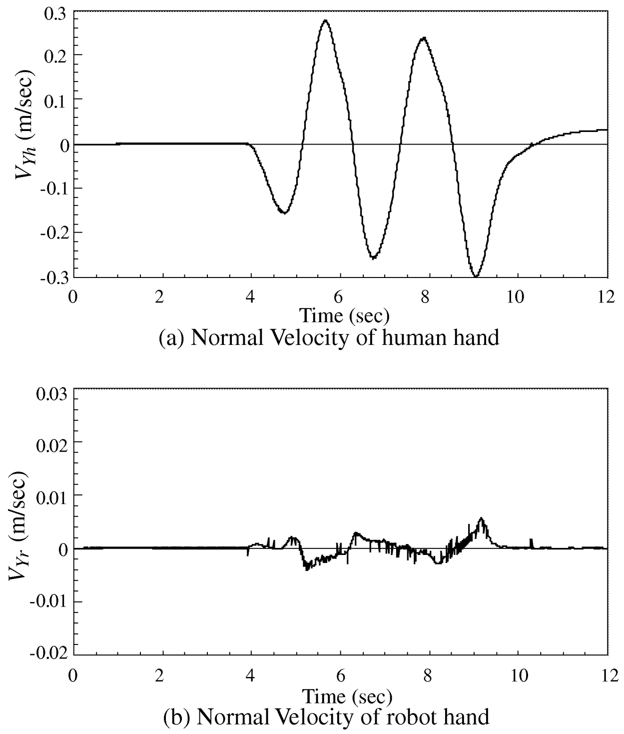

(a) Normal Velocity of human hand

(b) Normal Velocity of robot hand

Fig. 10: Sideslip with virtual nonholonomic constraint

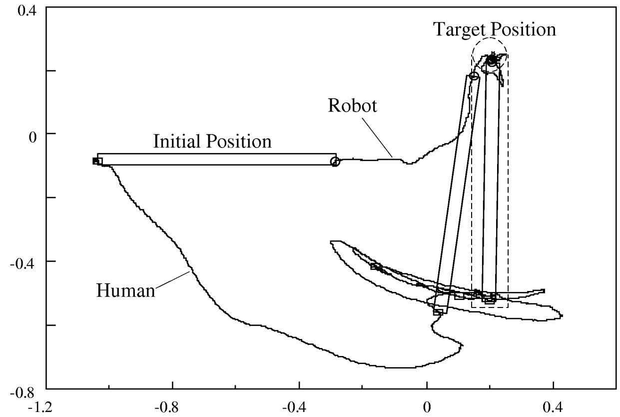

Fig. 11: Trajectory of object without torque (impedance control)

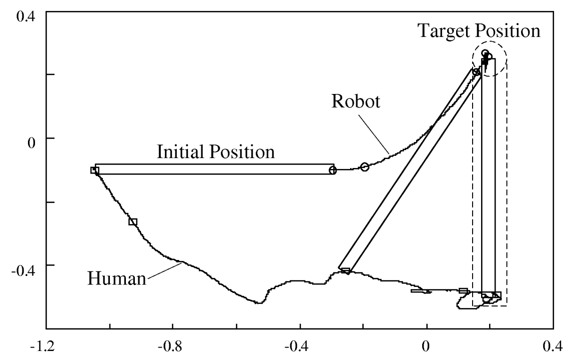

Fig. 12: Trajectory of object without torque (virtual nonholonomic constraint)

In the positioning task, complicated movements are required to control the sideslip of the object when using impedance control (**Fig. 11**). It is also difficult to correct small errors and stop the object accurately at the target position. On the other hand, the object can be easily positioned at the desired configuration with the virtual nonholonomic constraint (**Fig. 12**).

3 Six Degree-of-freedom Cooperative Manipulation in Three-dimensional Space

In this section, we extend the method described in Section **2** for cooperative manipulation to 3-D space. In our previous by reported method for manipulation in a vertical plane [9], it was difficult to change the inclination of the object. The robot raised or lowered its hand following the operator, and the object was maintained in a horizontal position.

The virtual nonholonomic constraint in 3-D space enables us to change the object's posture and to reach any position and orientation in 6-dof. First we will consider the simple case of cooperative handling in a vertical plane. We will demonstrate that the human operator can change the height of the object by using the virtual nonholonomic constraint. Then we will combine the constraints in the horizontal motion and the vertical motion for transporting the object in 3-D space. Finally, we will implement the control law to a real robot and demonstrate that a human and the robot can cooperatively carry a long object in 3-D space.

3.1 Cooperative manipulation in a vertical plane

Here we consider the motion in a vertical plane using the virtual nonholonomic constraint, so that the object can reach any desired position and inclination. In this method the operator can manipulate the object using skills similar to steering a wheelbarrow on a horizontal plane. Though the object cannot be lifted vertically, it can be positioned to a desired position along an appropriate trajectory.

A virtual constraint equivalent to a wheel is given to the robot hand (**Fig. 13**). The operator's holding point H is,(x_h, z_h), the robot's holding point R is,(x_r, z_r) . The object length is L and its inclination is θ_Y. The nonholonomic constraint which prevents the virtual wheel from slipping sideways is represented as

$$\dot{x}_r \sin\theta_Y - \dot{z}_r \cos\theta_Y = 0. \qquad (15)$$

The object can translate only in the axial direction, and it can rotate around R on the vertical plane. The controllability is guaranteed, based on nonholonomy as used in a horizontal plane.

We use the same method as in a horizontal plane to achieve the nonholonomic constraint at the robot hand. Frame (X, Z) is defined as in **Fig. 13**, and impedance control is applied to each axis as follows.

$$\begin{cases} f_{Xr} &= m_X \dot{v}_{Xr} + b_X \dot{v}_{Xr} \\ f_{Zr} &= m_Z \dot{v}_{Zr} + b_Z \dot{v}_{Zr} \\ \tau_{Yr} &= i_Y \ddot{\theta}_Y + c_Y \dot{\theta}_Y. \end{cases} \qquad (16)$$

m_Z and b_Z are large values set for the constraint, and m_X, b_X, i_Y and c_Y are small values set for the smooth movement. Then the virtual nonholonomic constraint equivalent to a wheel attached to the object is achieved in the vertical plane.

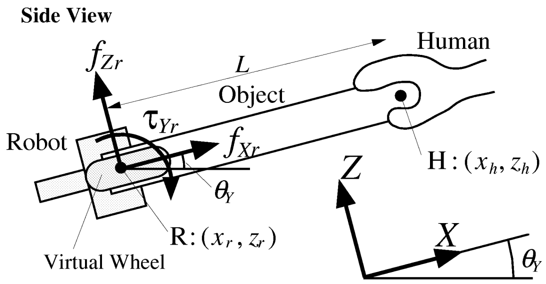

Fig. 13: Nonholonomic constraint in vertical plane.

Table 2: **Impedance parameters for vertical plane**

m_X	[kg]	5.5
b_X	[kg/s]	20
m_Z	[kg]	100
b_Z	[kg/s]	5000
i_Y	[kg m^2]	5.5
c_Y	[kg m^2/s]	20

From Eq.(16), the acceleration of the robot hand is obtained as

$$\begin{cases} \dot{v}_{Xr} &= (f_{Xr} - b_X v_{Xr})/m_X \\ \dot{v}_{Zr} &= (f_{Zr} - b_Z v_{Zr})/m_Z \\ \ddot{\theta}_{Yr} &= (\tau_{Yr} - c_Y \dot{\theta}_Y)/i_Y. \end{cases} \qquad (17)$$

The reference velocity $(v_{XrREF}, v_{ZrREF}, \dot{\theta}_{YrREF})$ of the robot hand is obtained by integrating Eq.(17) and is used for the velocity servo control.

Here we consider the load sharing, assuming that both holding points are free rotation pivots. The operator and the robot share the gravitational load in inverse proportion to the distance from the center of gravity. When the mass distribution of the object is uniform and its center of gravity is located at the midpoint, the operator and the robot share the load equally regardless of the object's mass and length.

We will demonstrate that a human and a robot can transport a long object to a desired height and inclination in a vertical plane. We used the same experimental setup as in Section **2.3.** A personal computer (CPU:PentiumIII, 550MHz) was used for the controller. The sampling time was 2 msec. The object was an aluminum pipe (Length: 0.75 m, Mass: 0.7 kg). The operator transports the object to the target position while watching the reference on a monitor screen. The impedance parameters employed in the experiments are listed in **Table 2.** When using the

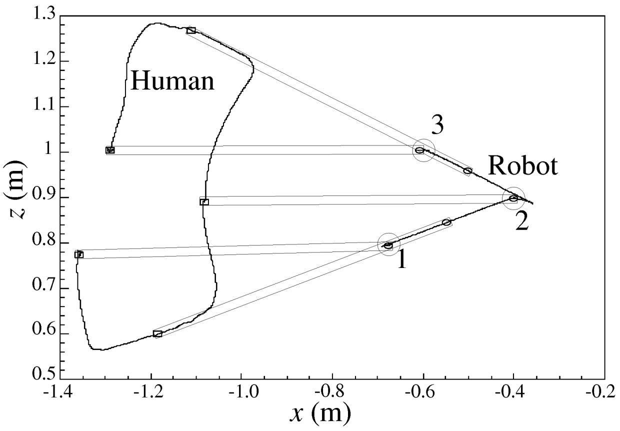

Fig. 14: Trajectory of object (virtual nonholonomic constraint).

nonholonomic constraint, the mass and friction coefficients in the normal direction were defined about 20 and 250 times larger than those in the axial direction.

Figure 14 shows an example of the transport. Since the robot hand has the nonholonomic constraint, the object cannot be raised directly in a perpendicular direction. Instead, the operator can incline the object about the robot hand and can move the object up or down only by pushing or pulling it in the axial direction. Though the direction of the local movement is restricted, this method does not decrease the degrees of freedom of the transportation in the vertical plane. The human operator can understand the object's behavior in the vertical plane and can transport it smoothly to the desired position.

3.2 Cooperative manipulation in 3-D space

3.2.1 Nonholonomic constraint in 3-D space

In this section we will combine the control law in both horizontal and vertical planes to achieve cooperative transport in 3-D space. The constraint in the horizontal and vertical planes has been defined in the robot hand coordinates. First, we consider simply combining these two motions in the hand frame (**Fig. 15**). In this method, the object translation in the Y-, Z-directions and rotation around the X-axis in the hand coordinates are inhibited. Thus, we must control the object's position and inclination in the 3-D space by moving it in the X-direction and rotating it around the Y- and Z-axes.

Here we focus on the composite rotation in 3-D

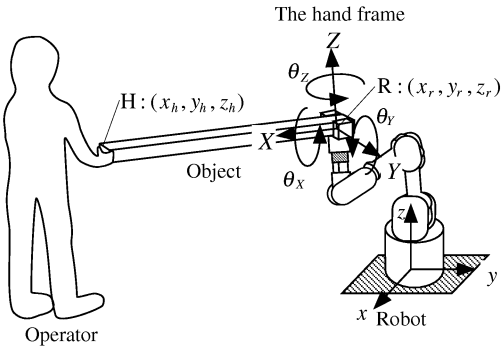

Fig. 15: Rotation about hand frame.

space by rotating the object around the Y- and Z-axes. We will describe the coordinates in 3-D space using the Z-Y-X Euler angles hereafter. We assume that the initial hand frame coincides with the absolute frame. In this orientation, θ_X is the Roll angle, θ_Y is the Pitch angle, θ_Z is the Yaw angle.

When we rotate the object initially around the Z-axis by α and then rotate it around the Y-axis by β, this rotation is represented by the following angles.

$$\theta_Z = \alpha, \theta_Y = \beta, \theta_X = 0. \tag{18}$$

We can see that the rotation around the X-axis does not occur. On the other hand, when we rotate the object initially around the Y-axis by β and then rotate it around the Z-axis by γ, this rotation is represented by the following angles.

$$\left\{ \begin{array}{lcl} \theta_Z &=& Atan2(\sin\gamma, \cos\beta\cos\gamma) \\ \theta_Y &=& Atan2(\sin\beta\cos\gamma, \sqrt{(\cos\beta\cos\gamma)^2 + (\sin\gamma)^2}) \\ \theta_X &=& Atan2(\sin\beta\sin\gamma, \cos\beta). \end{array} \right. \tag{19}$$

The object twists around the X-axis while rotating about the Y- and Z-axes. Since a human does not usually experience such object behavior, the transport task becomes difficult if the operator must always consider the order of the rotation axes in the hand frame and control the Roll angle by rotating around Y- and Z-axes. Thus, we consider the method that controls the twist around the X-axis for easier manipulation.

To manipulate in the horizontal or the vertical planes, the object is rotated around an axis normal to each plane. However, in 3-D space, the rotation axes are usually slanted relative to the absolute frame. Thus, rotation about the Y- and Z-axes affects other orientation angles like the above example.

To solve this problem, we propose a method in which the human operator directly controls the Roll

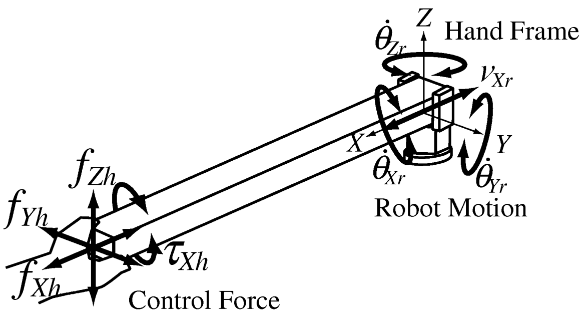

Fig. 16: Control Force and Robot Motion.

angle by twisting the object about the X-axis. This would allow the operator to adjust the object angle around the X-axis at will. To achieve the nonholonomic constraint, we restrict the translation in the Y- and Z-direction, and the object can translate in the X-direction and rotate around X-, Y- and Z-axes. In this method, the operator uses 3 translational forces in the X-, Y- and Z-direction and torque around the X-axis (**Fig. 16**). The object motion is described by nonholonomic kinematic model as an airplane or an under water vehicle [11].

Up to now, we have assumed that it is difficult to apply torque to a long object to generate translational force at the other end. However, when the object is rigid, the torque around the X-axis applied at the one end is transmitted to the other end directly. So it is easy to apply torque around the X-axis at the robot hand.

3.2.2 Controllability in 3-D space

Here, we discuss the controllability of our proposed method. The operator holds the object at H:(x_h, y_h, z_h) . The position and the Z-Y-X Euler angles of the robot hand R are $(x_r, y_r, z_r, \theta_Z, \theta_Y, \theta_X)$. The length of the object is L. When θ_Y is $\pm\,\pi/2$, it becomes the Z-Y-X Euler angles' singularity. However, we assume that the object safely avoids this singularity. The conditions in which the robot hand does not slip in the directions of the Y- and Z-axes are

$$\begin{aligned} &\dot{x}_r(\sin\theta_Z\cos\theta_Y) \\ &+\dot{y}_r(\sin\theta_Z\sin\theta_Y\sin\theta_X-\cos\theta_Z\cos\theta_X) \\ &+\dot{z}_r(\sin\theta_Z\sin\theta_Y\cos\theta_X-\cos\theta_Z\sin\theta_X)=0, \end{aligned} \tag{20}$$

$$-\dot{x}_r\sin\theta_Y+\dot{y}_r\cos\theta_Y\sin\theta_X+\dot{z}_r\cos\theta_Y\cos\theta_X=0. \tag{21}$$

The robot and human holding positions are related as

$$\left\{\begin{array}{l} x_h{=}L\cos\theta_Z\cos\theta_Y+x_r \\ y_h{=}L\sin\theta_Z\cos\theta_Y+y_r \\ z_h{=}{-}L\sin\theta_Y+z_r. \end{array}\right. \tag{22}$$

Differentiating Eq.(22), the relation of the velocities is as follows

$$\left\{\begin{array}{l} \dot{x}_h{=}{-}L\dot{\theta}_Z\sin\theta_Z\cos\theta_Y-L\dot{\theta}_Y\cos\theta_Z\sin\theta_Y+\dot{x}_r \\ \dot{y}_h{=}{-}L\dot{\theta}_Z\cos\theta_Z\cos\theta_Y-L\dot{\theta}_Y\sin\theta_Z\sin\theta_Y+\dot{y}_r \\ \dot{z}_h{=}{-}L\dot{\theta}_Y\cos\theta_Y+\dot{z}_r. \end{array}\right. \tag{23}$$

The state equation of this system is obtained from Eqs.(20), (21) and (23).

$$\begin{aligned} \begin{pmatrix} \dot{x}_r \\ \dot{y}_r \\ \dot{z}_r \\ \dot{\theta}_Z \\ \dot{\theta}_Y \end{pmatrix} &= \boldsymbol{R}_T\begin{pmatrix} \dot{x}_h \\ \dot{y}_h \\ \dot{z}_h \end{pmatrix} \\ &= \boldsymbol{g}_1\dot{x}_h+\boldsymbol{g}_2\dot{y}_h+\boldsymbol{g}_3\dot{z}_h. \end{aligned} \tag{24}$$

Where the matrix $\boldsymbol{R}_T$ is 5×3, the vectors $\boldsymbol{g}_1$, $\boldsymbol{g}_2$ and $\boldsymbol{g}_3$ are 5×1 as follows,

$$\left\{\begin{array}{lcl} \boldsymbol{g}_1 &=& \frac{\cos\theta_Y\cos\theta_Z}{D}(A,B,C,E,F)^T \\ \boldsymbol{g}_2 &=& \frac{\cos\theta_Y\sin\theta_Z}{D}(A,B,C,E,G)^T \\ \boldsymbol{g}_3 &=& -\frac{\sin\theta_Y}{D}(A,B,C,J,K)^T, \end{array}\right. \tag{25}$$

where A, B, C, D, E, F, G, J and K are

$$\left\{\begin{array}{lcl} A &=& \cos\theta_Y\cos\theta_Z(\cos^2\theta_X-\sin^2\theta_X) \\ B &=& \cos\theta_X\sin\theta_Z-\sin\theta_X\sin\theta_Y\cos\theta_Z \\ C &=& \cos\theta_X\sin\theta_Y\cos\theta_Z-\sin\theta_X\sin\theta_Z \\ D &=& A\cos\theta_Y\cos\theta_Z+B\cos\theta_Y\sin\theta_Z+C\sin\theta_Y \\ E &=& \frac{C}{L\cos\theta_Y} \\ F &=& \frac{C\sin\theta_Y\sin\theta_Z-B\cos\theta_Y}{L\cos^2\theta_Y\cos\theta_Z} \\ G &=& \frac{D+C\sin\theta_Y\sin^2\theta_Z-B\cos\theta_Y\sin\theta_Z}{LB\cos^2\theta_Y\cos theta_Z\sin\theta_Z} \\ J &=& -\frac{C\sin\theta_Y+D}{L\cos\theta_Y\sin\theta_Y} \\ K &=& \frac{B\cos\theta_Y-\sin\theta_Z(D+C\sin\theta_Y)}{L\cos^2\theta_Y\cos\theta_Z}. \end{array}\right. \tag{26}$$

Equation(24) is a drift-free affine system with the configuration of the object as the state variable and the translational velocities of H as the control inputs.

Now we will prove this system is controllable and can reach any arbitrary state [10]. Lie brackets of the vector fields $\boldsymbol{g}_1$, $\boldsymbol{g}_2$ and $\boldsymbol{g}_3$ are defined as,

$$\left\{\begin{array}{lcl} [\boldsymbol{g}_1;\boldsymbol{g}_2] &=& \frac{\partial\boldsymbol{g}_2}{\partial\boldsymbol{q}}\boldsymbol{g}_1-\frac{\partial\boldsymbol{g}_1}{\partial\boldsymbol{q}}\boldsymbol{g}_2 \\ [\boldsymbol{g}_2;\boldsymbol{g}_3] &=& \frac{\partial\boldsymbol{g}_3}{\partial\boldsymbol{q}}\boldsymbol{g}_2-\frac{\partial\boldsymbol{g}_2}{\partial\boldsymbol{q}}\boldsymbol{g}_3 \\ [\boldsymbol{g}_3;\boldsymbol{g}_1] &=& \frac{\partial\boldsymbol{g}_3}{\partial\boldsymbol{q}}\boldsymbol{g}_1-\frac{\partial\boldsymbol{g}_3}{\partial\boldsymbol{q}}\boldsymbol{g}_1. \end{array}\right. \tag{27}$$

This is calculated using the numerical calculation software "Mathematica" as follows.

$$rank(\boldsymbol{g}_1, \boldsymbol{g}_2, \boldsymbol{g}_3, [\boldsymbol{g}_1, \boldsymbol{g}_2], [\boldsymbol{g}_2, \boldsymbol{g}_3], [\boldsymbol{g}_3, \boldsymbol{g}_1]) = 5. \quad (28)$$

As the matrix $(\boldsymbol{g}_1, \boldsymbol{g}_2, \boldsymbol{g}_3, [\boldsymbol{g}_1, \boldsymbol{g}_2], [\boldsymbol{g}_2, \boldsymbol{g}_3], [\boldsymbol{g}_3, \boldsymbol{g}_1])$ is of full rank from Eq.(28), the system Eq.(24) satisfies Lie algebra rank condition, and it is controllable. It is possible to control the position (x_r, y_r, z_r) and posture (θ_Y, θ_Z) of the object only by treating the translational velocity of the operator's holding position. Finally, the rotation about the X-axis (θ_X) is controllable, because it is controlled directly by the operator's torque about the X-axis (τ_{Xh}).

3.2.3 Anisotropic impedance control in 3-D space

Now we will explain the robot controller used to implement our proposed method to the robot arm. The robot has a force sensor at the wrist. We consider the frame of the robot hand in **Fig. 15** and use impedance control for each axis of the following impedance characteristics.

$$\begin{cases} f_{Xr} &= m_X \dot{v}_{Xr} + b_X \dot{v}_{Xr} \\ f_{Yr} &= m_Y \dot{v}_{Yr} + b_Y \dot{v}_{Yr} \\ f_{Zr} &= m_Z \dot{v}_{Zr} + b_Z \dot{v}_{Zr} \\ \tau_{Xr} &= i_X \ddot{\theta}_{Xr} + c_X \dot{\theta}_{Xr} \\ \tau_{Yr} &= i_Y \ddot{\theta}_{Yr} + c_Y \dot{\theta}_{Yr} \\ \tau_{Zr} &= i_Z \ddot{\theta}_{Zr} + c_Z \dot{\theta}_{Zr}. \end{cases} \quad (29)$$

$(f_{Xr}, f_{Yr}, f_{Zr}, \tau_{Xr}, \tau_{Yr}, \tau_{Zr})$ are force and torque, $(v_{Xr}, v_{Yr}, v_{Zr}, \dot{\theta}_{Xr}, \dot{\theta}_{Yr}, \dot{\theta}_{Zr})$ are velocity and angular velocity, $(\dot{v}_{Xr}, \dot{v}_{Yr}, v_{Zr}, \ddot{\theta}_{Xr}, \ddot{\theta}_{Yr}, \ddot{\theta}_{Zr})$ are acceleration and angular acceleration, $(m_X, m_Y, m_Z, i_X, i_Y, i_Z)$ are inertia and moment of inertia and $(b_X, b_Y, b_Z, c_X, c_Y, c_Z)$ are viscous friction and moment of viscous friction. The impedance parameters of the Y- and Z-axes were set large to achieve the constraint Eqs.(20) and (21). Small X-axis and rotational parameters were given so that the object could be moved more easily by the operator's force.

From Eq.(29), the acceleration and the angular acceleration of the robot arm is

$$\begin{cases} \dot{v}_{Xr} &= (f_{Xr} - b_X v_{Xr})/m_X \\ \dot{v}_{Yr} &= (f_{Yr} - b_Y v_{Yr})/m_Y \\ \dot{v}_{Zr} &= (f_{Zr} - b_Z v_{Zr})/m_Z \\ \ddot{\theta}_{Xr} &= (\tau_{Xr} - c_X \dot{\theta}_{Xr})/i_X \\ \ddot{\theta}_{Yr} &= (\tau_{Yr} - c_Y \dot{\theta}_{Yr})/i_Y \\ \ddot{\theta}_{Zr} &= (\tau_{Zr} - c_Z \dot{\theta}_{Zr})/i_Z. \end{cases} \quad (30)$$

Integrating Eq.(30), the reference velocities of the robot hand are obtained. The reference velocities are converted into the joint angular velocity and given to the servo system of each joint. Thus, the control system of the virtual nonholonomic constraint can be realized in 3-D space.

Table 3: **Impedance parameters for 3-D space**

m_X	[kg]	5.5
b_X	[kg/s]	20
m_Y	[kg]	100
b_Y	[kg/s]	5000
m_Z	[kg]	100
b_Z	[kg/s]	5000
i_X, i_Y, i_Z	[kg m^2]	5.5
c_X, c_Y, c_Z	[kg m^2/s]	20

3.3 Experiment in 3-D space

We demonstrated that a human and robot can transport a long object to a desired position and posture in 3-D space. We used the same experimental setup as in Section **2.3**. **Table 3** shows the impedance parameters. The mass and friction parameters in the constraint axes were defined about 20 and 250 times larger than those in the unconstrained axes. The operator and the robot transport the object cooperatively to the target position from the initial position. The initial and target positions of the robot are $(x_r, y_r, z_r, \theta_X, \theta_Y, \theta_Z)$ = (-0.47, -0.47, 0.37, 0.0, 0.0, 0.0), (0.35, 0.2, 0.63, 0.0, 0.0, $\pi/2$) in the absolute coordinate, respectively.

Figure 17 shows a picture of the experiment. **Figure 18** shows the experimental result with rotation about the Y- and Z-axes. **Figure 19** shows the experimental result with rotation about the X-, Y- and Z-axes. **Figure 20** shows the rotational angle about the X-axis in each experiment. The rotation about the Y- and Z-axes results in rotation about the X-axis during transport to the target position. The operator cannot understand how the object's posture changes, and it is too difficult to reach the desired angle only by rotation about the Y- and Z-axes. On the other hand, the result of rotation about the X-, Y- and Z-axes is that the operator can easily control the Roll angle about the X-axis and the object can reach the target position and posture. This result shows that our proposed method can accomplish cooperative manipulation with 6 degrees of freedom in 3-D space.

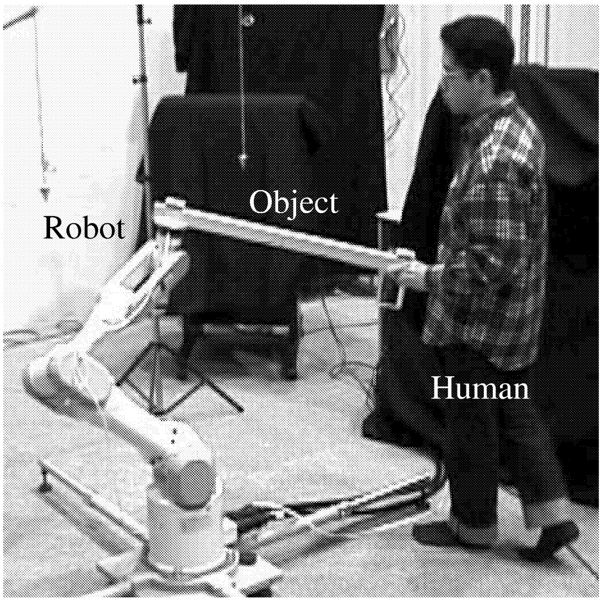

Fig. 17: Experiment of 3-D transportation.

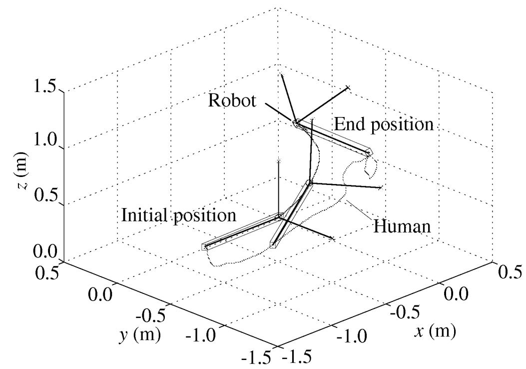

Fig. 18: Experimental result (Rotation about Y,Z-axis).

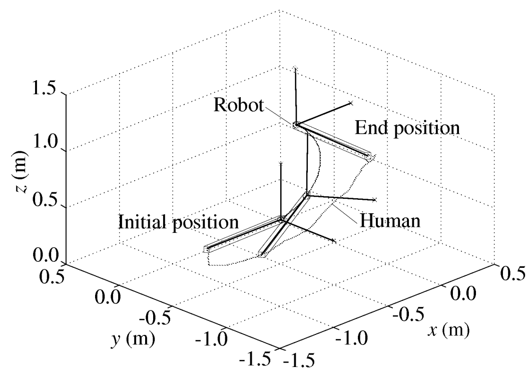

Fig. 19: Experimental result (Rotation about X,Y,Z-axis).

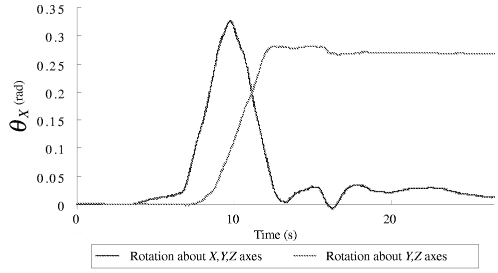

Fig. 20: Rotation angle about X-axis.

4 Conclusions

We proposed a method which enables a human and a robot to support each end of a long object and manipulate it cooperatively. The robot is given a virtual nonholonomic constraint equivalent to a wheel attached to the object in the axial direction. This method allows the object to be moved to an arbitrary position and orientation while preventing sideslip. The constraint is achieved using anisotropic impedance control in the hand frame.

We first used this method in the horizontal plane. Those experimental results show that the operator could easily understand the behavior of the object and that cooperative handling could be simplified. Next, we extended the concept of virtual nonholonomic constraint to motion in the vertical plane, and we combined the horizontal motion and vertical motion for 6-dof manipulation in 3-D space. The operator could transport the object to an arbitrary position and posture in 3-D space with skills similar to using a wheelbarrow. We thus verified the effectiveness of our proposed method experimentally.

References

[1] H. Kazerooni, "Human Robot Interaction via the Transfer of Power and Information Signals," IEEE Trans. Systems, Man and Cybernetics, Vol. 20, No. 2, pp.450–463, 1990.

[2] K. Kosuge, Y. Fujisawa and T. Fukuda, "Mechanical System Control with Man-Machine-Environment Interactions," Proc. 1993 IEEE Int. Conf. on Robotics and Automation (ICRA'93), pp.239–244, 1993.

[3] Y. Hayashibara, K. Tanie, H. Arai and H. Tokashiki, "Development of Power Assist System

with Individual Compensation Ratios for Gravity and Dynamic Load," Proc. 1997 IEEE Int. Conf. on Intelligent Robots and Systems (IROS'97), pp.640–646, 1997.

[4] W. Wannasuphoprasit, R. Gillespie, J. E. Colgate and M. Peshkin, "Cobot control," Proc. of 1997 IEEE Int. Conf. on Robotics and Automation (ICRA'97), pp. 3571–3576, 1997.

[5] K. M. Lynch and C. Liu, "Designing Motion Guides for Ergonomic Collaborative Manipulation," Proc. of 2000 IEEE Int. Conf. on Robotics and Automation (ICRA'00), pp. 2709–2715, 2000.

[6] K. Kosuge, H. Yoshida and T. Fukuda, "Dynamic Control for Robot-Human Collaboration," IEEE Int. Workshop on Robot and Human Communication, pp.398–401, 1993.

[7] R. Ikeura and H. Inooka, "Variable Impedance Control of a Robot for Cooperation with a Human," Proc. 1995 IEEE Int. Conf. on Robotics and Automation (ICRA'95), pp.3097–3102, 1995.

[8] O. M. Al-Jarrah and Y. F. Zheng, "Arm-Manipulator Coordination for Load Sharing Using Reflexive Motion Control," Proc. 1997 IEEE Int. Conf. on Robotics and Automation (ICRA'97), pp.2326–2331, 1997.

[9] Y. Hayashibara et al., "Assist System for Carrying a Long Object with a Human - Analysis of a Human Cooperative Behavior in the Vertical Direction -," Proc. 1999 IEEE Int. Conf. on Intelligent Robots and Systems (IROS'99), pp.695–700, 1999.

[10] R. M. Murray, Z. Li and S. S. Sastry, *A Mathematical Introduction to Robotic Manipulation*, CRC Press, 1993.

[11] Y. Nakamura, S. Savant, "Nonholonomic Motion Control of an Autonomous Underwater Vehicles," Proc. 1991 IEEE Int. Conf. on Intelligent Robot and Systems(IROS'91), pp.1254–1259, 1991.

[12] H. Arai, T. Takubo, K. Tanie, "Human-Robot Cooperative Manipulation Using a Virtual Nonholonomic Constraint," Proc. 2000 IEEE Int. Conf. Robotics and Automation (ICRA'00), pp.4064–4070, 2000.

[13] T. Takubo, H. Arai, K. Tanie, "Virtual Nonholonomic Constraint for Human-Robot Cooperation in 3-D space," Proc. 2000 IEEE Int. Conf. on Intelligent Robots and Systems (IROS'00), pp.300–305, 2000.

[14] T. Takubo, H. Arai, K. Tanie : "Human-Robot Cooperative Handling Using Virtual Nonholonomic Constraint in 3-D space", Proc. 2001 IEEE Int. Conf. Robotics and Automation (ICRA'01), pp.2680–2685, 2001.